

The resistive switching (RS) conduction characteristics of $\text{La}_{1-x}\text{Sr}_x\text{MnO}_3$ (LSMO) films grown by the Chemical Solution Deposition (CSD) method were investigated [1]. In particular, in this work, we focused the attention on the partial resets that arise from the application of successive voltage ramps of increasing magnitude. Remarkably, most published works on the RS behavior of LSMO deal with the bistable behavior rather than with the progressive reset curves. The I-V characteristics are simulated using a nonlinear memristive approach based on the double-diode equation:

$$I = \text{sgn}(V)[(\alpha R)^{-1} W\{\alpha R I_0 \exp[\alpha(|V| + R I_0)]\} - I_0]$$

in combination with the solution of the generalized logistic differential equation (curve Γ^+ in Fig.1) [3]

$$\frac{d\Gamma}{dV} = \eta \Gamma^{1+\beta(1-\gamma)} (1 - \Gamma^\beta)^\gamma$$

which has sigmoidal shape with parameters β , γ , and η . W is the Lambert function. The parameters I_0 , α , and R are driven by the solid trajectories shown in Fig.1 according to the relationship $\Omega = \Omega_m + \lambda(\Omega_M - \Omega_m)$, where $\Omega = (I_0, \alpha, R)$. Ω_m and Ω_M are the minimum and maximum values of Ω , respectively [2]. $0 < \lambda < 1$ is the state variable and describes the fraction of active conducting channels/volume at time t . The I-V curves corresponding to the complete increasing and decreasing voltage sequence are illustrated in Fig. 2. Two representations are used for the same data (linear-linear and log-linear). Notice the good agreement between experimental and model results in both scales. The external I-V loop is used to calibrate the model parameters.

References

- [1] C. Moreno et al. Nano Lett., vol. 10, no. 10, pp. 3828–3835, (2010)
- [2] M. Krasnosel'skiĭ and A. Pokrovskiĭ, Systems with hysteresis, Springer
- [3] A. Tsoularis, Res. Lett. Inf. Math. Sci. 2, pp. 23-46 (2001)

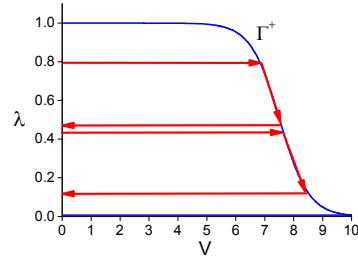


Figure 1: Hysteretic trajectories for the reset I-V characteristics

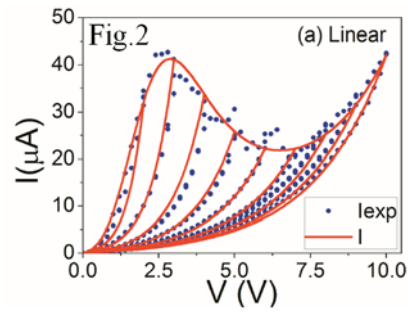


Figure 2: Experimental and model results in linear-linear scale

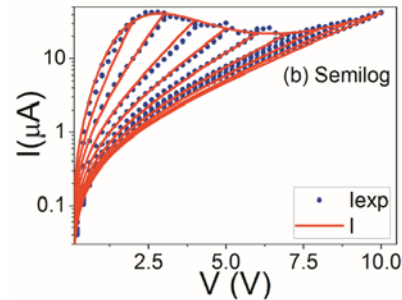


Figure 3: Experimental and model results in log-linear scale